7-11

SANDIA REPORT

SAND95–1201 • UC–401
Unlimited Release
Printed June 1995

Trapping of Radiation in Plasmas

Merle E. Riley, W. Joseph Alford

Prepared by
Sandia National Laboratories
Albuquerque, New Mexico 87185 and Livermore, California 94550
for the United States Department of Energy
under Contract DE-AC04-94AL85000

SF2900Q(8-81)

Issued by Sandia National Laboratories, operated for the United States Department of Energy by Sandia Corporation.

Available to DOE and DOE contractors from
Office of Scientific and Technical Information
PO Box 62
Oak Ridge, TN 37831

Prices available from (615) 576-8401, FTS 626-8401

Available to the public from
National Technical Information Service
US Department of Commerce
5285 Port Royal Rd
Springfield, VA 22161

NTIS price codes
Printed copy: A03
Microfiche copy: A01

SAND95-1201
Unlimited Release
Printed June 1995

Distribution
Category UC-401

Trapping of Radiation in Plasmas

Merle E. Riley
and
W. Joseph Alford
Laser, Optics, and Remote Sensing Department
Sandia National Laboratories
Albuquerque, NM 87185-1423

Abstract

We analyze the problem of radiation trapping (imprisonment) by the method of Holstein. The process is described by an integrodifferential equation which shows that the effective radiative decay rate of the system depends on the size and the shape of the active medium. Holstein obtains a global decay rate for a particular geometry by assuming that the radiating excited species evolves into a steady state spatial mode. We derive a new approximation for the trapped decay which has a space dependent decay rate and is easy to implement in a detailed computer simulation of a plasma confined within an arbitrary geometry. We analyze the line shapes that are relevant to a near-atmospheric-pressure mixture of He and Xe. This line-shape analysis can be utilized in either the Holstein formulae or the space-dependent decay approximation.

Contents **Page**

1. Introduction

Radiation emitted within an optically thick system is partially reabsorbed before it exits the physical volume of the system. The effect is very important when the transition connects to the ground level of the emitting species or to a highly populated metastable level. The effect has been found to be important in discharge lamps. The Hg emissions of fluorescent lamps is a notable example from the lighting industry.[1,2] The prime system of interest to us is the operation of discharge flat panel display panels[3] in which the density of the ground level atoms is usually large enough to result in trapping of the ultraviolet emission that is used to excite the phosphors. Generally one cannot construct an adequate theoretical model of the discharge kinetics in any of these systems unless the trapping is included in the rate equations. Radiation trapping leads to a decrease in the emission rate and a change in the spectral density within the line profile. Early work on radiation trapping attempted a diffusion analysis of the absorption-reemission process of radiation transport within the system. T. Holstein[4,5] (referred to as TH) pointed out that a diffusion limit of the transport equation was *not* correct for *any* of the common line shapes. References to the earlier work are given in TH. TH showed that the effective decay rate of the radiatively trapped system depends on the geometry of the active volume. The TH analysis assumes complete line redistribution within the absorption-reemission process, which means that the emission profile is the same as the absorption profile. This may not be true in all circumstances, but appears to be valid for most systems[4].

Holstein has developed analytic formulae for the effective decay rates of pressure-broadened and Doppler-broadened lines, with the active volume either an infinite plane-parallel slab[1] or cylinder.[2] The cylinder is of special importance in the analysis of fluorescent lights. The TH analysis consists of two basic parts. First of all, one obtains the correct form of the integral equation for radiation transport within the medium, and, second, the spatial profile of the emitting species is assumed to be controlled by the decay process itself. TH finds the spatial mode for each geometry by a variational approximation.

There are *three* fundamental difficulties with use of the TH results. The first is contained in the line shapes: if the line profile is not purely Doppler broadened (Gaussian profile) or pressure broadened (typically a Lorentz profile), then one must decide which region of the line dominates the radiation leakage from the system. Huennekens and Colbert[6] have shown that using the larger of the escape factors of a pure Doppler or pure pressure broadened line (when both mechanisms

are active) agrees with their experimental results. They refer to other discussions of this point. The second difficulty in using the TH results is that an actual system may not be a slab or a cylinder. Although the shape dependence is weak, being mainly a function of the smallest dimension, this is a basic limitation of the analytic results. The third problem with the TH study is that the spatial profile of the emitting species is constrained to be that of the fundamental mode of the decaying excited level. Van Trigt[7] develops higher modes of the basic transport equation, but our main concern is that other competing kinetic processes within the system are just as fast as the *trapped* decay rate and that the radiating mode may never be established. All these difficulties will be addressed in this report. In particular we will derive a formula for a space dependent decay rate that has a simple dependence on geometry.

We mention that there is a new series of computational solutions to radiation trapping and transport that rely on full numerical solutions of the radiation spectral transport equations.[8,9] This is the method of choice for an accurate examination of the coupled kinetics and radiation evolution of a discharge plasma. The only difficulty is that the radiation transport part of the problem makes it difficult to implement implicit numerical methods in the discharge simulations. For this reason we are pursuing applications of the TH theory to situations of different geometry and transient time dependence. These results will be easy to incorporate into an existing discharge simulation code.

2. Analysis of Radiation Transport and Trapping

In this Section 2. we will write down the basic equations for radiation transport in a medium with the presence of trapping. The first Subsection 2.1 will present the basic equations and review the results of TH. Next in Section 2.2 we will demonstrate the lack of applicability of the diffusion equation to trapping by a novel approach. Subsection 2.3 will present a new approximation for the integrodifferential equation for transport. Lastly in Subsection 2.4 we will use an approximate analysis based on the transmission functions of TH[4,5] to determine the space-dependent decay rate within the active medium.

If the reader is just interested in implementing the TH theory, then they can proceed directly to Section 3 after reviewing Section 2.1.

2.1 Review of Trapping and the TH Results

In this section we will write down the basic equations that describe radiation transport within a gas that possesses complete spectral redistribution.[4] Most of these relations are contained in TH. First consider the photon (radiation) space and spectral density, $n(\vec{r}, \nu, t)$, produced by upper level emission and lower level absorption. The upper level number density is n_u, and the lower level density is n_l. All of these quantities are space and time dependent with the only restriction being that changes are slow on the scale of the radiation transit time of the medium. Later we will incorporate the requirement that the active medium is contained within a volume V with absorbing walls, within which the lower level density is uniform and constant, and the upper level has an unspecified form. We have in general the expression for the photon density:

$$n(\vec{r},\nu,t) = \int d^3r' \frac{1}{4\pi|\vec{r}-\vec{r}'|^2}\frac{1}{c}\gamma_{sp}P(\nu)n_u(\vec{r}',t) \times \exp\left(-\sigma(\nu)\int_0^{|\vec{r}-\vec{r}'|} ds\, n_l(\vec{r}'+s\hat{e}(\vec{r},\vec{r}'),t)\right). \quad (1)$$

If n is multiplied by $h\nu$ and integrated over frequency, we have the radiation energy density. In Eq.(1) c is the speed of light, γ_{sp} is the spontaneous decay rate, and

$$
\begin{aligned}
k(\nu) &= \kappa P(\nu) = \sigma(\nu) n_l \,, \\
&\int_{-\infty}^{\infty} d\nu P(\nu) = 1, \\
&\vec{s} = \vec{r} - \vec{r}' \,, \\
&\hat{e}(\vec{r}, \vec{r}') = \vec{s} \,/\, s \,.
\end{aligned}
\tag{2}
$$

$k(\nu)$ is the extinction of the radiation at frequency ν due to absorption by the lower level, $P(\nu)$ is the normalized emission profile related to the extinction because of the redistribution assumption, and $\sigma(\nu)$ is the absorption cross section. The transition rate of the upper level number density at position $\vec{r}$ due to radiative decay and absorption is

$$
\dot{n}_u(\vec{r}, t) = -\gamma_{sp} n_u(\vec{r}, t) + \int d\nu c \, \sigma(\nu) n(\vec{r}, \nu, t) n_l(\vec{r}, t). \tag{3}
$$

Stimulated emission and changes in n_l are not important in these systems because of the large population of the lower level. Eqs.(1) and (3) can be combined into the transport equation for the number density of the upper level:

$$
\dot{n}_u(\vec{r}, t) = -\gamma_{sp} n_u(\vec{r}, t) + \gamma_{sp} \int d^3 r' G(\vec{r}, \vec{r}', t) n_u(\vec{r}', t). \tag{4}
$$

where

$$
\begin{aligned}
G(\vec{r}, \vec{r}', t) &= \frac{1}{4\pi\rho^2} n_l(\vec{r}, t) \int d\nu P(\nu) \sigma(\nu) \exp\left(-\sigma(\nu) \int_0^s ds' \, n_l(\vec{r}' + s'\hat{e}, t) \right), \\
s &= \left| \vec{r} - \vec{r}' \right|.
\end{aligned}
\tag{5}
$$

It is reasonable to assume that the number density of the lower level is constant within a convex active volume *V*, and with time, in which case Eq.(5) can be more simply written:

$$G(\vec{r},\vec{r}',t)=G(|\vec{r}-\vec{r}'|)=\frac{1}{4\pi s^2}\int_{-\infty}^{\infty} dv\,P(v)k(v)\exp(-k(v)s), \qquad (6)$$
$$\vec{r},\vec{r}' \in V .$$

The convex condition ensures that the path integral in Eq.(5) remains within the volume V as long as the end points are within V. The integration over all space must now be restricted to the integration over V, since the spatial dependence of n_l has been lost. It is sometimes advantageous to express G(s) as a derivative of the transmission function T(s):

$$G(s)=-\frac{1}{4\pi s^2}\frac{d}{ds}T(s),$$
$$T(s)=\int_{-\infty}^{\infty} dv\,P(v)\exp(-k(v)s), \qquad (7)$$
$$T(0)=1 .$$

T(s) is the probability that the radiation, weighted by the emission profile, is not absorbed after travelling a distance s from the emission point. If one can evaluate the function T(s), or G(s), then the integrodifferential Eq.(4) is available to solve for the upper level density and decay.

The equation that we have obtained is for the upper level atomic number density. An analogous equation can be written for the first spectral-weighted moment, $n_1(\vec{r},t)$, of the photon density:

$$\dot{n}_1(\vec{r},t)=-\gamma_{sp}\,n_1(\vec{r},t)+\gamma_{sp}\int_V d^3r'\,G(s)\,n_1(\vec{r}',t),$$
$$n_1(\vec{r},t)=\int dv\,P(v)\,n(\vec{r},v,t). \qquad (8)$$

Thus the moment of the radiation spectral distribution obeys the same transport equation as the upper level density. This is different than the spectral average.

Expressions for T(s) have been obtained by TH for the Doppler line shape, the impact pressure broadened line (Lorentz), and the quasi-static (statistical) pressure broadened line. Only the Lorentz line has an exact result, the others

being asymptotic forms that apply for large extinction. For completeness, we write down some of those results. The Doppler line profile is

$$
\begin{aligned}
k(\nu) &= k_o \exp\left(-((\nu-\nu_o)/\nu_o)^2\,(c/\mathrm{v_o})^2\right), \\
\mathrm{k_o} &= \frac{\lambda_o{}^3 n_l}{8\pi}\frac{g_u}{g_l}\frac{\gamma_{sp}}{\sqrt{\pi}\mathrm{v}_o}, \\
\mathrm{v_o} &= \sqrt{2kT/M}, \\
\Delta\nu_{fwhm} &= \sqrt{4\ln 2}\,\nu_o\,\mathrm{v}_o/c.
\end{aligned}
\tag{9}
$$

The notation is standard, involving wavelength, degeneracy ratio, mass, and thermal velocity. TH evaluates the asymptotic form of T(s), namely,

$$
T(s) \sim 1/k_o s\sqrt{\pi\ln(k_o s)}\,. \tag{10}
$$

The impact line profile is, ignoring the line shift term[5]:

$$
\begin{aligned}
k(\nu) &= k_p \frac{1}{1+(4\pi(\nu-\nu_o)/\gamma_p)^2}, \\
k_p &= \frac{\lambda_o{}^2 n_l}{2\pi}\frac{g_u}{g_l}\frac{\gamma_{sp}}{\gamma_p}, \\
\Delta\nu_{fwhm} &= \gamma_p/2\pi,
\end{aligned}
\tag{11}
$$

where γ_p is the pressure broadened FWHM in 1/s. γ_p is directly proportional to the collision frequency. T(s) can be evaluated exactly, namely,

$$
\begin{aligned}
T(s) &= I_o(k_p s/2)\exp(-k_p s/2), \\
&\sim 1/\sqrt{\pi k_p s}, \quad large\ k_p s\,.
\end{aligned}
\tag{12}
$$

Only the asymptotic result was written down in TH. I_o is the modified Bessel function of order zero.

The procedure in TH is to use Eqs.(10) or (12) in the variational approximation to evaluate the spatial profile of the emitting level within either an

infinite slab or an infinite cylinder. From this approximation one derives an "escape factor", g, that relates the decay rate of the approximated fundamental spatial mode of Eq.(4) to the spontaneous rate: $\gamma_{eff} = g\,\gamma_{sp}$. Again from TH, these results are listed here for the two distinct line profiles and the two geometries. In all cases the asymptotic, large-extinction, limit is used.

First TH gives the impact broadened (ib) case (Lorentz profile) in a slab of thickness L and a cylinder of radius R:

$$\begin{aligned} g_{ib,slab} &= 1.150 / \sqrt{\pi k_p L}\,, \\ g_{ib,cyl} &= 1.115 / \sqrt{\pi k_p R}\,. \end{aligned} \tag{13}$$

Next the Doppler broadened (db) case, again in a slab of thickness L and a cylinder of radius R:

$$\begin{aligned} g_{db,slab} &= 1.875 / k_o L\sqrt{\pi \ln(k_o L)}\,, \\ g_{db,cyl} &= 1.60 / k_o R\sqrt{\pi \ln(k_o R)}\,. \end{aligned} \tag{14}$$

These are the main results of TH, except for the algebraically more complex quasi-static broadening case, which we will not present in detail.

An interesting observation concerning the TH results in Eqs.(13)-(14) is that the g factors are close to being the value of the transmission function *T(s)* with *s* evaluated at the "middle" of the volume, *ie* either *s* = R for the cylinder or *s* = L/2 for the slab. In fact, for the four cases in Eqs.(13)-(14), the functional form is that of T(s) and the numerical coefficients differ by factors of 0.813, 1.115, 0.938, and 1.60,. We have ignored the small variation produced by the log term in the Doppler case.[4,5] Only the *g* value of the Doppler-broadened cylinder is significantly different than unity. These factors directly enable us to express *g* in terms of *T*. This suggests that we may obtain a simple approximate connection of *g* to *T* for more than just the TH geometries.

There appears to be agreement in the literature[6,10,11] that a line shape with both Doppler and pressure-broadened regions (for example, a Voigt profile) can be analyzed with the TH results. The procedure is to find the frequency at which the extinction through the medium is unity, and to use the trapping formula for Doppler or impact cases depending whether the unit-trapping frequency lies in the

Doppler or impact region of the composite line shape. The Huennekens-Colbert procedure[6] appears to logically and smoothly combine these ideas by choosing the larger of the g factors for the different line profiles for a particular geometry. We will discuss and use this procedure in Section 3.

2.2 Study of the Diffusion Limit of the Integral Equation

The integrodifferential Eq.(4) complicates the numerical simulation of plasmas. Typically all of the operators in a plasma particle simulation are local in space, with only the boundary conditions for the Poisson equation forcing a nonlocal character. By local, one means that the time derivatives for the dependent variables in the differential equations of motion are expressible in terms of function values or spatial differential operators at the same point in space. For one thing, this facilitates implicit numerical time incrementation. It is obvious that a replacement of the integral operator in Eq.(4) with a local operator, say the diffusion Laplacian, would greatly lessen the difficulty of the computation. The early studies of the diffusion "approximation" to radiation transport neglected some crucial analysis that is necessary to find an effective diffusion coefficient.[4] The work of TH showed that "infinities" would arise with the assumption of a diffusion description of the emission and absorption process for the common line shapes involved in atomic systems. In this section we analyze the diffusion limit *quantitatively* from the view of Fourier transform theory.

We will convert Eq.(4) from coordinate space to transform space. Define a general space transform and its inverse by:

$$\begin{aligned} \tilde{n}(\vec{k}) &= \int d^3r\, n(\vec{r}) \exp(-i\vec{k}\cdot\vec{r}) \,, \\ n(\vec{r}) &= (2\pi)^{-3} \int d^3k\, \tilde{n}(\vec{k}) \exp(i\vec{k}\cdot\vec{r}) \,. \end{aligned} \tag{15}$$

The time variable will be suppressed in writing the equations in this section. The integrals cover all space, with any finite boundaries incorporated by the properties of $n(\vec{r})$. Define:

$$D(\vec{r}-\vec{r}') = \gamma_{sp}\left(-\delta^3(\vec{r}-\vec{r}') + G(|\vec{r}-\vec{r}'|\right), \tag{16}$$

which allows us to write the transform of the integrodifferential Eq.(4):

$$\dot{\tilde{n}}(\vec{k}) = \tilde{D}(k)\tilde{n}(\vec{k}). \tag{17}$$

Here the transform of the kernel is:

$$\begin{aligned}\tilde{D}(k) &= -\gamma_{sp}\left(1+\int_0^\infty dx \frac{\sin(kx)}{kx}\frac{dT(x)}{dx}\right) \\ &= -\gamma_{sp}\int_0^\infty dx\, T(x) k\, j_1(kx) \\ &= -\gamma_{sp}\int_0^\infty dz\, T(z/k) j_1(z)\end{aligned} \tag{18}$$

all of which is deceptively simple, but nevertheless does aid the diffusion analysis. T is just the transmission function of scalar argument as defined in Eq.(7). j_1 is the spherical Bessel function of order one, which is a simple function of sines and cosines.

Now, a diffusion limit, if it exists, will give rise to an equation in transform space of the form:

$$\dot{\tilde{n}}(\vec{k}) = -D_f k^2 \tilde{n}(\vec{k}), \tag{19}$$

where D_f is the diffusion constant. The second power of k corresponds to the Laplacian operator. The notion of locality arises in the sense of $n(\vec{r})$ being spatially smooth and thus $\tilde{n}(\vec{k})$ localized in $\vec{k}$ space about zero. Thus the function $\tilde{D}(k)$ is only needed *near* zero values of the magnitude of k, and may be expanded in a power series in k. A complementary view of locality may be expressed in coordinate space in terms of the peaked nature of G(s) and the smoothness of the densities.

If the transmission function is an exponential, $T(s) = \exp(-s/d)$, we find that

$$\tilde{D}(k) = -\gamma_{sp}\left(1-\frac{\arctan(kd)}{kd}\right),$$
$$= -\gamma_{sp}\frac{(kd)^2}{3}, \quad kd \to 0. \tag{20}$$

This is the standard diffusion result, proportional to k^2, depending on the radiation mean free path.

Our task is to find the small-k limit of Eq.(18); this is straightforward from the second expression in the group:

$$\tilde{D}(k) \xrightarrow[k\to 0]{} -\gamma_{sp}\frac{1}{3}k^2\int_0^\infty dx\, T(x)x. \tag{21}$$

However this expression is indeterminate if the forms of $T(x)$ for the Doppler or Lorentz line are substituted from Eqs.(10) or (12). The appropriate well defined limit is found from the last expression in Eq.(18). Using the Lorentz form given in Eq.(12), we find:

$$\tilde{D}(k) \xrightarrow[k\to 0]{} -\gamma_{sp}\int_0^\infty dz \frac{\sqrt{k}}{\sqrt{\pi k_p z}} j_1(z)$$
$$= -\gamma_{sp}\frac{1}{3}\sqrt{\frac{2k}{k_p}}. \tag{22}$$

Thus the transform-space limit that should lead to the k^2 dependence and the diffusion form leads instead to a fractional power of k and an ill-defined inverse transform in coordinate space. There may exist some useful inverse to the $\sqrt{k}$ dependence in coordinate space, but we have not found it.

It is instructive to understand why a diffusion description fails for our radiation transport problem. Note that we are not claiming failure because of the finite size of the container, which could occur for any transport problem with a large mean free path between scattering events, but a failure in principle due to the process itself. Since each frequency obeys Beer's law (exponential decrease with distance), one might expect that a diffusion description would follow in the

appropriate limit just as it does for particle propagation. The crucial difference is that we have assumed, more or less correctly, that the radiation transport possesses complete frequency redistribution for each absorption-emission process. The summation over all frequencies leads to a transport Eq.(4), which does not obey Beer's law as evidenced by Eqs.(10) or (12), and a failure of the diffusion equation to apply with any size container.

To reiterate the results of this section, the lack of a k^2 dependence of $\tilde{D}(k)$ as $k \to 0$ proves that the diffusion equation cannot be rigorously derived from the radiation transport equation. Only if the integral appearing in Eq.(21) is finite can one infer a diffusion constant for the transport. Modifications to the basic form of *T(s)*, such as introducing a cutoff to give convergence,[12] may be successful, but one would have to establish that the radiative emission from the medium (decay rate) is not a sensitive function of the cutoff point. Another possible route to forcing a diffusion approximation is to equate the TH decay rate for the fundamental mode of Eq.(4) to the decay rate of the fundamental diffusion mode, and in so doing, fix an empirical diffusion constant. This is a geometry-specific result, but it should be reasonably accurate.

2.3 Approximation of Integral Equation by Local Operator

In order to construct an approximation for the integral operator that represents the radiation reabsorption in Eq.(4), one must look for a procedure that takes advantage of the spatially singular nature of the kernel G(s) at s=0, but also does not neglect the long range character at large s. Let us rewrite Eq.(4) in its general form:

$$\dot{n}_u(\vec{r},t) = -\gamma_{sp} \int_V d^3r' \left(\delta^3(\vec{r}-\vec{r}') - G(|\vec{r}-\vec{r}'|)\right) n_u(\vec{r}',t). \qquad (23)$$

We now integrate over the volume to find the total decay rate of all upper levels within the medium:

$$N_u(t) = \int_V d^3r\, n_u(\vec{r},t),$$

$$\dot{N}_u(t) = -\gamma_{sp} \int_V d^3r' \left(1 - \int_V d^3r\, G(|\vec{r}-\vec{r}'|)\right) n_u(\vec{r}',t). \qquad (24)$$

As may be shown from Eq.(7), the integral over all space of *G(s)* is unity for any positive amount of extinction in the system. Thus one minus the integral over d^3r in the last equation may be replaced by an integral over the space *external* to the active volume if we agree to define the constant lower level density throughout all space. Nothing within the active volume is changed - only the range of definition of the function *G(s)*. This leaves:

$$\begin{aligned} \dot{N}_u(t) &= -\gamma_{sp} \int_V d^3r'\, g(\vec{r}')\, n_u(\vec{r}',t), \\ g(\vec{r}) &= \int_{Vext} d^3r'\, G(|\vec{r}-\vec{r}'|). \end{aligned} \tag{25}$$

The first equation can be interpreted as the integration over the active medium of *an effective decay rate* of the upper level at that point in space, namely:

$$\gamma_{eff}(\vec{r}) = \gamma_{sp}\, g(\vec{r}). \tag{26}$$

The determination of g is yet to be accomplished, but it will develop that it can be reasonably approximated using the results of TH.

As a systematic means of leading to this approximation for the radiation transport, return to the exact Eq.(23) and introduce an expansion for the upper level density under the integral. An analysis of the kernel shows that the most important contribution to the integral arises from positions near to the point $\vec{r}$. This suggests that we expand in a Taylor series:

$$\begin{aligned} \dot{n}_u(\vec{r},t) &= \int_V d^3r' D(\vec{r}-\vec{r}')\left(n_u(\vec{r},t) + (\vec{r}'-\vec{r})\cdot\vec{\nabla} n_u(\vec{r},t) + \cdots\right) \\ &= n_u(\vec{r},t)\int_V d^3r' D(\vec{r}-\vec{r}') + \vec{\nabla} n_u(\vec{r},t)\cdot\int_V d^3r'(\vec{r}'-\vec{r})\, D(\vec{r}-\vec{r}') + \cdots, \end{aligned} \tag{27}$$

where D is defined in Eq.(16). Truncating this series at the leading term leads to the "local" approximation for the transport equation:

$$\dot{n}_u(\vec{r},t) \cong n_u(\vec{r},t) \int_V d^3r' D(\vec{r}-\vec{r}') . \qquad (28)$$

The local description applies because the density has effectively been removed from the integral and evaluated at the position $\vec{r}$. We see that the previous interpretation of Eq.(26) applies to Eq.(28) with the identical definition of $g(\vec{r})$, giving :

$$\dot{n}_u(\vec{r},t) \cong -\gamma_{sp}\, g(\vec{r})\, n_u(\vec{r},t) . \qquad (29)$$

The function $g(\vec{r})$ depends on the size and shape of the active medium because we have assumed that the lower level is uniformly distributed throughout V. $g(\vec{r})$ does not depend on the distribution of the upper level density within V. However, our new approximation becomes *exact* only as the upper level density becomes uniform within the active volume *V*.

The time dependent behavior of the solution to Eq.(29) is that of an exponentially decaying initial upper level density with a space-dependent decay rate. The solution does *not* settle into a fundamental eigenmode of the transport Eq.(4) where the solution decays in time with a single overall rate. Eq.(29) is most accurate, as mentioned, when the upper level density is nearly uniform within V. This is a transient situation requiring an eigenmode superposition as developed by van Trigt[7] as an extension of the TH analysis. Moreover, the situation of a decaying prepared initial upper level density should be contrasted with the case of a *uniform source* of upper level excitation by other kinetic processes, in which the TH analysis predicts a spatially *uniform* density of upper levels at steady state, whereas Eq.(29) will predict a spatial profile dependent on $g(\vec{r})$. This seems more realistic.

2.4 Determination of the Localized Decay Rate

The whole point of this subsection in the calculation of the position-dependent scale factor g connecting the effective decay rate to the spontaneous emission rate as defined in Eqs.(25) and (26). The precise expression for g is:

$$g(\vec{r}) = \int_{Vext} d^3r' G(|\vec{r} - \vec{r}'|) = \int_{Vext} d^3r' G(s)$$
$$= \int_{Vext} d^3r' \frac{-1}{4\pi s^2} \frac{dT(s)}{ds}. \qquad (30)$$

Of course $s = |\vec{r} - \vec{r}'|$ in these expressions. Note that, by writing g as an integral over the external volume to the medium, we have maintained additivity in the joining of exterior volume pieces around the medium. We wish to approximate g in a very general manner so that the size and shape dependence of the effective decay rate is preserved. The g integral has a simple geometrical interpretation that is worth describing. If we change from integration variable $\vec{r}'$ to $\vec{s} = \vec{r}' - \vec{r}$, and express the boundaries of the volume in terms of the new variables, we have:

$$g(\vec{r}) = \int_{Vext} d^3s G(s)$$
$$= \int_{Vext} d^3s \left(\frac{-1}{4\pi s^2} \frac{dT(s)}{ds} \right)$$
$$= \int_0^\infty s^2 ds \left(\frac{-1}{4\pi s^2} \frac{dT(s)}{ds} \right) \int_{Vext} d^2s$$
$$= -\int_0^\infty ds \frac{dT(s)}{ds} \Theta(s, \vec{r}) \qquad (31)$$
$$= \int_0^\infty ds T(s) \frac{\partial \Theta(s, \vec{r})}{\partial s}.$$

$\Theta(s, \vec{r})$ is the fraction of the solid angle subtended by the *exterior* space at the distance s from the point $\vec{r}$ in the medium. Thus $\Theta(s, \vec{r})$ is zero for s less than the minimum distance to a boundary, and is unity for s greater than the span of the medium. In writing the last expression in Eq.(31) we have assumed that the point $s = 0$ lies within the medium and that $\Theta(0, \vec{r})$ is zero there. This is only important in obtaining limiting results at the surface of the medium.

2.4.1 The Semi-infinite Volume and Infinite Slab Geometries

An explicit evaluation of Eq.(31) is possible in idealized conditions. Consider the point $\vec{r}$ to lie at a distance z measured into a medium bounded by an infinite plane boundary. Then the function $\Theta(s,\vec{r})$ is found to be:

$$\begin{aligned} \Theta(s,z) &= 0, \quad s \le z, \\ \Theta(s,z) &= \tfrac{1}{2}(1 - z/s), \quad s > z, \\ \partial\Theta(s,z)/\partial s &= 0, \quad s \le z, \\ \partial\Theta(s,z)/\partial s &= z/2s^2, \quad s > z. \end{aligned} \tag{32}$$

Later we will approximate g for general T, but here we will evaluate g for the specific geometry taking advantage of the TH analytic forms of the transmission function. The effective decay factor g can be evaluated using Eq.(12) for the impact broadening (ib) case in the semi-infinite volume (∞):

$$\begin{aligned} g_{ib,\infty}(z) &= \int_z^\infty ds\, T(s) \frac{\partial\Theta(s,z)}{\partial s} \\ &\cong \int_z^\infty ds \min\left(1, \frac{1}{\sqrt{\pi k_p s}}\right) \frac{z}{2s^2} \\ &= \tfrac{1}{3}/\sqrt{\pi k_p z}, \quad \pi k_p z > 1, \\ &= \tfrac{1}{2} - \tfrac{1}{6}\pi k_p z, \quad \pi k_p z < 1. \end{aligned} \tag{33}$$

In Eq.(33) we have used a simple bounding relation to make the asymptotic form of Eq.(12) acceptable for the whole range of s. One might equally well have used the asymptotic form of T for all s within the integral over s and applied the upper bound of 1/2 (radiating source at surface of medium) to the g value. For the Doppler-broadened (db) case we use the asymptotic form of T and do the integral by pulling out the slowly varying log factor. The result is:

$$g_{db,\infty}(z) \sim \tfrac{1}{4}/k_o z\sqrt{\pi \ln(k_o z)}. \tag{34}$$

Of course this function must be bounded as $z \to 0$; the appropriate bound is 1/2, so one can just use the minimum of the function value as given in Eqs.(34) and 1/2 as a reasonable evaluation of the function for any value of the argument z.

The case of a plane parallel slab is just the sum of Eq.(33), or of Eq.(34), with $z = z_1$ and $z = z_2$ where z_1 and z_2 are the distances from the two plane boundaries of the slab. For impact broadening:

$$g_{ib,slab}(z_1, z_2) = \min\left(\tfrac{1}{2}, \tfrac{1}{3} / \sqrt{\pi k_p z_1}\right) + \min\left(\tfrac{1}{2}, \tfrac{1}{3} / \sqrt{\pi k_p z_2}\right) , \tag{33a}$$

and for Doppler broadening,

$$g_{db,slab}(z_1, z_2) = \min\left(\tfrac{1}{2}, \tfrac{1}{4} / k_o z_1 \sqrt{\pi \ln(k_o z_1)}\right) + \min\left(\tfrac{1}{2}, \tfrac{1}{4} / k_o z_2 \sqrt{\pi \ln(k_o z_2)}\right) . \tag{34a}$$

We have chosen the simpler method of correcting the asymptotic forms as discussed following Eq.(34) above.

It is interesting to compare to the TH result for the decay of the fundamental mode, which is peaked in the center of the slab and decreases towards the edges. If we set $z_1 = z_2 = L/2$ in Eq.(33a) to correspond to the center, we obtain:

$$g_{ib,slab} \sim 0.943 / \sqrt{\pi k_p L} , \tag{35}$$

which is 18% less than the TH result in Eq.(14), but remember that we are looking at the slowest of our position-dependent decay rates at the center of the slab and comparing to the TH decay for the whole mode. For the Doppler case in Eq.(34a) we get:

$$g_{db,slab} \sim 1 / k_o L \sqrt{\pi \ln(k_o L / 2)} . \tag{36}$$

This is a factor of 1.85 smaller than TH, but the same rationale applies as mentioned after Eq.(35).

2.4.2 Spherical Geometry

Another idealized geometry that can be explored is the spherical medium of radius R. Consider $\vec{r}$ to lie a distance z from the center, with z restricted to be in the range of 0 to R. The solid angle fraction and its derivative are:

$$\begin{aligned}
\Theta(s,z) &= 0, \quad s \le R - z, \\
\Theta(s,z) &= \frac{(z+s)^2 - R^2}{4zs}, \quad R - z < s < R + z, \\
\Theta(s,z) &= 1, \quad s \ge R + z, \\
\partial\Theta(s,z)/\partial s &= 0, \quad s \le R - z, \\
\partial\Theta(s,z)/\partial s &= \frac{s^2 + R^2 - z^2}{4zs^2}, \quad R - z < s < R + z, \\
\partial\Theta(s,z)/\partial s &= 0, \quad s \le R - z.
\end{aligned} \tag{37}$$

Although Θ is a continuous function of s, the derivative is not, and one must be careful in evaluating the irregular double limit of $z \to R$ and $s \to 0$ under the integral for $g(z)$, which is

$$\begin{aligned}
g(z) &= \int_{R-z}^{R+z} ds\, T(s) \frac{s^2 + R^2 - z^2}{4zs^2} \quad , \quad 0 \le z \le R, \\
&= 1 \quad , \quad T(s) = 1 \quad .
\end{aligned} \tag{38}$$

The decay factor is easy to evaluate at the center of the sphere, where the limit is:

$$g(0) = T(R). \tag{39}$$

The effective decay rate at the surface of the sphere may be found from Eq.(38). It is:

$$g(R) = \frac{1}{2}\left(1 + \frac{1}{2R}\int_0^{2R} ds\, T(s)\right). \tag{40}$$

Note that these results reduce to the proper value of unity when the transmission function is one. If we know a particular form for the line broadening, we can substitute *T(s)* into Eq.(38) and have a position-dependent decay rate for the spherical medium that is useful.

2.4.3 Recommendation for General Geometry

The question is what to do in general with the geometry factor. Are all geometries similar to a sphere or a slab? We think that sufficient insight may be gotten from those results to make a general statement possible. Consider the result of combining Eqs.(31) and (32) to find the decay rate in a semiinfinite medium at a distance z from a plane boundary:

$$g(z) = \tfrac{1}{2} z \int_z^\infty ds\, T(s) / s^2 \,. \tag{41}$$

If the extinction is large, that is to say in the asymptotic region where T behaves as in Eqs.(10) or (12), we can approximate the integral in Eq.(41) based on the slower variation of *T(s)* under the integral. This gives:

$$g(z) \cong \tfrac{1}{2} z\, T(z) \int_z^\infty ds / s^2 = \tfrac{1}{2} T(z) \,. \tag{42}$$

This result also happens to be exact ($g = 1/2$) in the limit that $T \to 1$ at small extinction within the medium. In the case of the sphere, we can apply the same argument based on the slow variation of T at larger extinction in order to approximate from Eq.(38):

$$
\begin{aligned}
g(z) &= \frac{1}{4z}\int_{R-z}^{R+z} ds\,T(s) + \frac{R^2-z^2}{4z}\int_{R-z}^{R+z} ds\,T(s)/s^2 \\
&\cong \frac{1}{4z}T(R)\int_{R-z}^{R+z} ds + \frac{R^2-z^2}{4z}T(R-z)\int_{R-z}^{R+z} ds/s^2 \qquad (43) \\
&= \tfrac{1}{2}T(R) + \tfrac{1}{2}T(R-z),
\end{aligned}
$$

where R is the radius of the spherical volume and z is the distance from the center. We note that Eq.(43) is also correct ($g = 1$) in the $T = 1$ limit of no extinction. It is exact at the center of the sphere as given in Eq.(39). It is also in reasonable agreement with the surface value calculated in Eq.(40).

Based on the form of the result in Eq.(43), what we propose for a general arbitrary geometry formulation of the effective decay rate is

$$
g(\vec{r}) = \tfrac{1}{2}T(R_o) + \tfrac{1}{2}T(d_{near}(\vec{r})), \qquad (44)
$$

where R_O is some fixed mean radius of the active volume and $d_{near}(\vec{r})$ is the distance from the point $\vec{r}$ to the *nearest* boundary surface of the volume. Note that *all* of the space dependence in g is contained in the transmission function to the nearest surface. The other term can be thought of as a normalization constant added in order to obtain the correct decay in the center of the medium. The definition of the mean radius is of concern when we apply Eq.(44) to the idealized infinite span geometries considered by TH. Next we will examine Eq.(44) with various limits and tests.

First of all, Eq.(44) reduces to the correct result of $g = 1$ everywhere within any shape volume for small extinction and little radiation trapping, where $T = 1$. It is also true that it approaches the correct value of 1/2 as the position $\vec{r}$ approaches any locally plane boundary of the volume for large extinction and trapping. The formula correctly reduces to Eq.(39) at the center of a spherical medium.

The infinite slab and cylinder of TH afford some insight into the mean radius, R_O. It would appear that we should choose R_O to be the largest radius sphere that fits *within* the active volume. Thus for the slab and cylinder with $\vec{r}$ positioned at the center, the two terms of Eq.(44) are equal, and Eq.(44) reduces to:

$$g_{slab}(center) = T(L/2),$$
$$g_{cyl}(center) = T(R). \tag{45}$$

TH's asymptotic formulae, Eqs.(13) and (14) for impact and Doppler broadening would have given, in terms of the T function:

$$g_{ib,slab} = 0.813\,T(L/2),$$
$$g_{ib,cyl} = 1.115\,T(R),$$
$$g_{db,slab} = 0.938\,T(L/2), \tag{46}$$
$$g_{db,cyl} = 1.60\,T(R).$$

This connection of g to the transmission function has been discussed previously in the text following Eq.(14). If the fixed radius R_O had been chosen larger, the first, fixed, term of Eq.(44) would be smaller and our approximations in Eq.(45) could be up to a factor of one half smaller. Since this does not improve the agreement with TH's results for the mode decay rate in Eq.(46), we feel that chosing R_O as the enclosed sphere's radius is adequate for active medium shapes that are not close to spherical.

We remind the reader that only a full numerical solution of the radiation transport equation with spectral redistribution is capable of reproducing subtleties in exotically shaped media.

It recently came to our attention that a series of articles by Irons[13] discusses the construction of the "escape factor" for radiation trapping. These articles are a good review of all of the work prior to 1978 on trapping, especially for analytic approximations. We should point out that our Eq.(44), which is being advanced for general geometries, appears to be unique among all approximations.

3. Broadening of the He and Xe Lines in a Mixture

The shape of spectral lines is an extremely complex subject even without the added complications of trapping of the radiation within an emitting volume, which has been the subject of the preceding material in this report. Fortunately we need only be concerned with some of the simpler issues[14] in the emission from mixtures of noble gas plasmas. Generally there are three mechanisms that contribute to the observed width in frequency of an untrapped spectral line: the natural width due to the finite lifetime of the emitting state, the Doppler width due to the distribution in velocities of the emitting species, and the collisional width due to interactions with other species. The natural width is generally unimportant at the temperatures and pressures of interest in our systems. However the natural line shape is Lorentzian, which decreases slowly in the wings of the profile, and therefore possibly important in situations of strong trapping as we will discuss in the following subsection. The trapping process strongly modifies the radiation line shape that escapes from an optically thick medium, but we will not be concerned with the emitted line profile. In the plasma flat panel display, the absorption of the emitted light is by a phosphor which is not sensitive to the profile.

3.1 Line Broadening in Trapped Emission

In the absence of trapping we do not have to be concerned with the shape of the emission line: the decay rate is that of spontaneous emission and the profile is broadened without affecting the rate. Trapping brings in the feature that the effective decay *rate* is a function of the line shape.[4,5] TH managed to evaluate the asymptotic forms of the transmission function (T(s) in Eq.(7)) only for the Doppler, Lorentzian, and quasi-static lines when they are pure. An examination of the transmission function integral by the saddle point method shows that the dominant contribution to the integral arises from frequencies in the neighborhood of the unit optical depth (UOD) point ν_x:

$$k(\nu_x)R_o = 1. \qquad (47)$$

In this determination of ν_x, one should think of R_O as being the characteristic radius R_O of the active volume as discussed in Section 2.4.3. It is interesting that a simple approximation of the transmission integral by an expansion of the exponentiated integrand through second power in frequency about the zero-

slope point agrees to within a factor of two with the exact results in the asymptotic region where the line center extinction is large. Thus there is little question that the behavior of trapped radiation should be governed by the line shape in the vicinity of the UOD point [6,10,11] via the transmission function of TH.

Any one of the three mechanisms (natural, Doppler, or collisional) could dominate the line shape in the neighborhood of the UOD point. TH points out that Doppler and collisional broadening both tend to have complete spectral redistribution in the absorption-emission process, whereas natural broadening does not possess complete redistribution. The question is how to cover all regions of broadening with a meaningful approximation based on the TH theory. The specific recommendation of Huennekens and Colbert[3] (their method 2) is to evaluate the trapped decay rates of TH for Doppler and collisional mechanisms (but not natural) and to choose the larger of the rates. They show that this method is much preferable by comparison to experiment on Na emission. This also avoids the use of the TH formulae for natural broadening where they were not intended. We have adopted the Huennekens and Colbert procedure in lieu of trying to calculate a *composite* line shape and to obtain a *new* approximation for the T integral.

The Doppler line profile is given in Eq.(9) and the Lorentzian line profile in Eq.(11). The Doppler effect by itself always produces the Gaussian shape as given in Eq.(9), but pressure or collisional broadening is not always of the Lorentzian shape, even if it is the only active mechanism for broadening. The Lorentzian profile arises from the so-called impact limit or phase interruption limit of collisional broadening in which the collisions of the radiating species are basicly short in duration and isolated in time. The condition for validity of the impact approximation is frequently expressed as $|\omega - \omega_o| << 1 / \tau_c$ where τ_c is the "duration" of the collision.[14] The other extreme of this limit, $|\omega - \omega_o| >> 1 / \tau_c$, gives rise to an approximation called quasi-static broadening (or sometimes the statistical model) and the line shape is no longer Lorentzian, being dependent on the form of the interaction potential between the emitter and perturber. The frequency profile of a line is not purely of any single form. The most common compound form is the Voigt profile resulting from the combined effect of Doppler and impact-limit broadening. The line center tends to appear Gaussian and the wings Lorentzian due to the slower decay with frequency.

Let us summarize what we need from the atomic physics in order to implement the calculation of the trapped decay rates from the plasma system. The

basic quantity to be determined is the transmisson function, T(s). The simplest approach is to assume that the active medium is close to a slab or a cylindrical geometry. In this case T(s), with s set to L/2 or R, can either be used directly in the TH formulae in Eq.(46), which are rewrites of Eqs.(13) and (14), to calculate the decay rate of the fundamental spatial mode. The more complicated approach is to use our newly derived space-dependent decay rate as formulated in Section 2.4.3 in Eq.(44), which requires T(s) as a function of s. Whichever method is used, we must construct T(s) for the radiative transition, which requires examination of the line shape in the neighborhood of the UOD point in order to determine the important line broadening mechanism.

3.2 The 147 nm Transition of Xe in He, Xe Mixtures

Here we must immediately specialize to a particular system, and if we are using the TH formulae, to a particular geometry. We choose a slab geometry with the gas at a temperature of 300 K and a thickness of $L = 100\,\mu m$. The Xe wavelength, frequency (in Hz), and radian frequency (in 1/s) are:

$$\begin{aligned} \lambda_o &= 147.0\,nm\,, \\ \nu_o &= c/\lambda_o\,, \\ \omega_o &= 2\pi\nu_o\,. \end{aligned} \tag{48}$$

We will assume a foreign gas pressure broadening coefficient of 10 MHz/Torr for He collisions with Xe, which is typical of this kind of transition and collision species, but the value is not precisely known. From this, of course, we find γ_p as present in Eq.(11) due to the collisions with He. This is only valid in the impact limit for frequencies nearer to line center and must be supplemented with the quasi-static broadening theory if we require the line shape very far from line center. The impact resonance broadening of excited Xe colliding with Xe is treated using the data of Carrington, Stacey, and Cooper.[15] This contributes to the Lorentz profile just as the usual impact broadening mechanism. The spontaneous decay rate, γ_{sp}, is set to 0.3 per ns.[16]

The UOD (unit optical depth) frequencies, $\omega_x = 2\pi\nu_x$ are examined by plotting the roots of Eq.(47) with $R_O = L$ for the extinctions as given in Eq.(9) for Doppler and in Eq.(11) for impact broadening for a fixed Xe pressure as a function of He pressure. The results at 1 Torr Xe are given in Fig. 1 and 10 Torr Xe in Fig. 2.

We have also included the quasi-static result for a van der Waals' interaction calibrated using the Weisskopf model[14] and our He-Xe foreign gas broadening coefficient of 10MHz/Torr. Because the TH theory does not treat a combination of broadening mechanisms, we do not have the ability to combine the quasi-static foreign broadening of He with Xe and the impact broadening of Xe on Xe. Thus the quasi-static UOD line does not include the Xe-Xe broadening, which would dominate at low He pressure. A rough estimate of the collision duration of He and Xe gives $1/\tau_c \approx 10^{12}/s$. Thus the impact theory should be good up to about 1 kTorr of He. The first observation from Figs. 1 and 2 is that radiation trapping with the Doppler line shape is dominated by much smaller frequencies (*ie*, closer to line center) than the pressure broadening cases. This means that we should use the trapped decay rates based on the impact or quasi-static line shapes for *total* gas pressures over a few Torr. The impact limit of the pressure broadening would appear to be valid over nearly the complete range of interest for plasma flat panel displays. At 10 Torr Xe, the information in Fig. 2 shows that the impact and quasi-static UOD frequencies are comparable at about 500 Torr of He, but this is of negligible effect up to 1000 Torr.

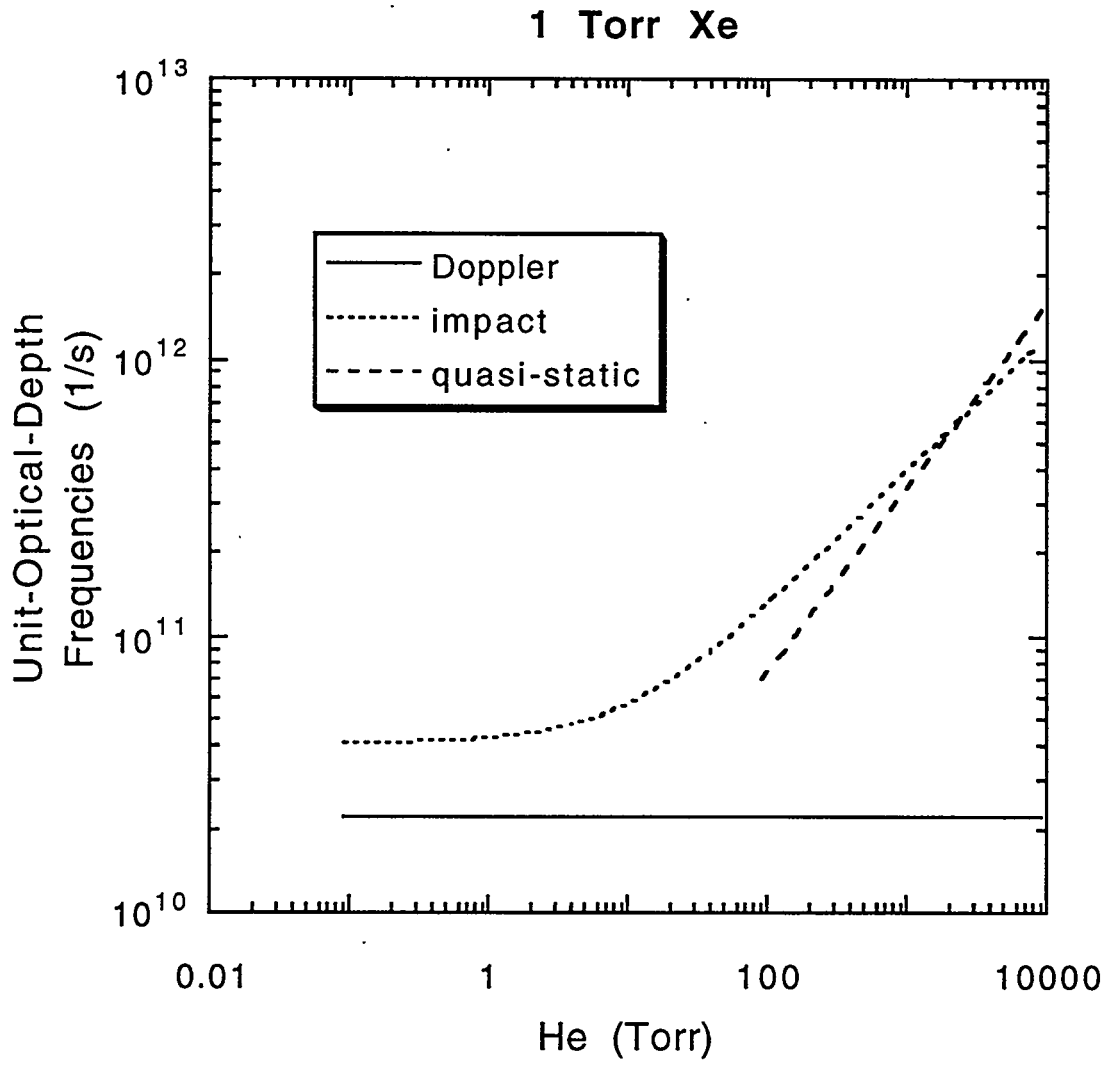

Figure 1. Variation of the UOD (unit optical depth) frequencies measured from line center as a function of He pressure for 1 Torr of Xe. The characteristic length is 100 μm in the evaluation of the optical depth. "impact" refers to the impact limit of the total Xe plus He and Xe plus Xe broadening, while "quasi-static" refers to the quasi-static line shape of the Xe plus He system.

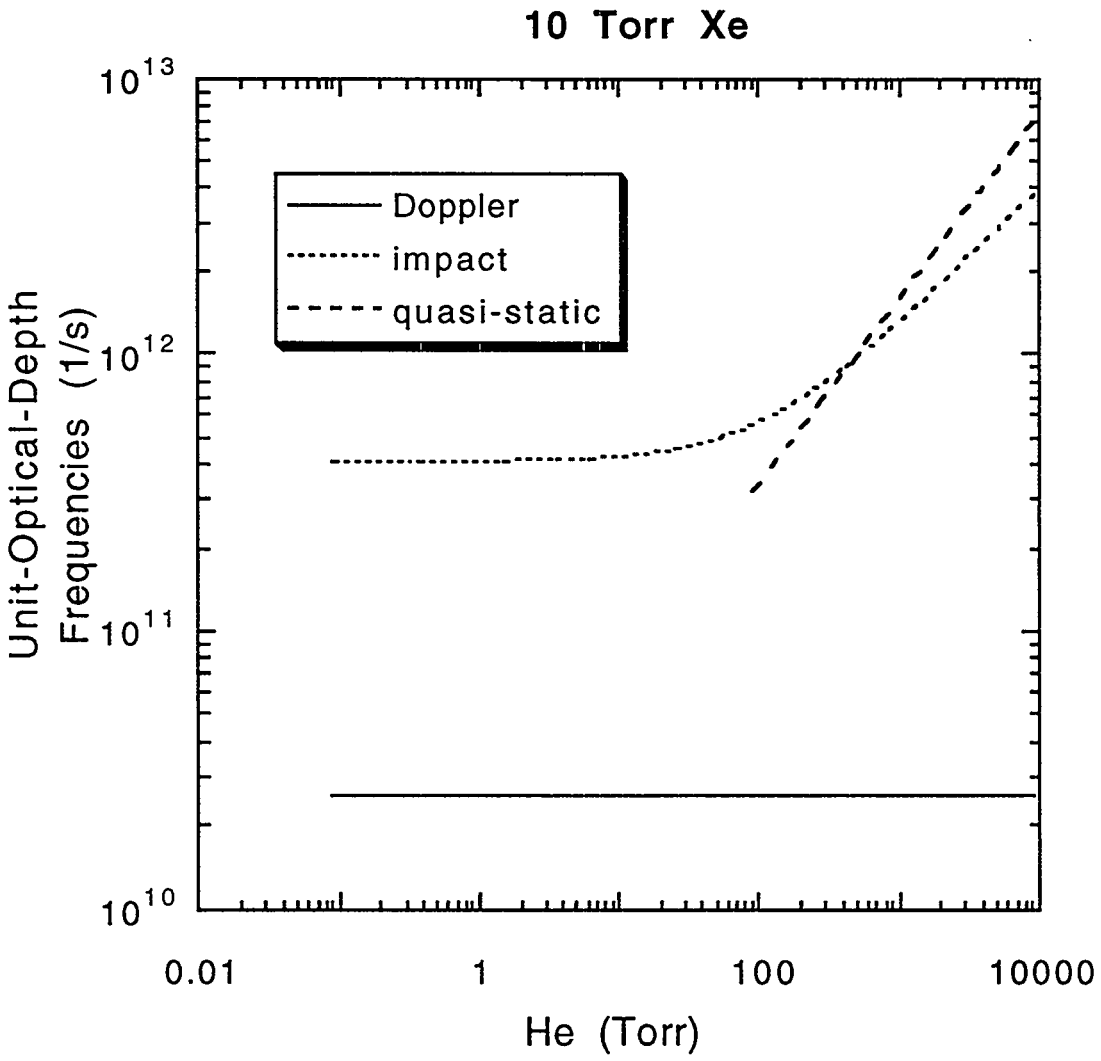

Figure 2. Variation of the UOD (unit optical depth) frequencies measured from line center as a function of He pressure for 10 Torr of Xe. The characteristic length is 100 μm in the evaluation of the optical depth. "impact" refers to the impact limit of the total Xe plus He and Xe plus Xe broadening, while "quasi-static" refers to the quasi-static line shape of the Xe plus He system.

Examination of the UOD tells us which line profile is most important in the region of frequency that escapes from the medium. An alternative procedure is to examine the transmission function evaluated for the different broadening mechanisms. In Figs. 3 and 4 we plot the escape factors for the different line shapes evaluated according the the TH formulae for the Xe and He case under study. According to the prescription of Huennekens and Colbert[6] we choose the largest of the escape factors (largest decay rate) as the correct simulation of the radiation trapping. It is to be noted that this is consistent with the UOD analysis in Figs. 1 and 2. By this we mean that the dominance of the pressure broadening over Doppler occurs for about the same pressure, and that the transition region from impact to quasi-static occurs at nearly the same pressure of He. Of course this is not fortuitous, as one can show that the analytic formulae must predict nearly the same results.

The above theory can be compared to experimental observations for trapping in pure Xe.[17] The experiments covered a pressure range of 0.002 to 10 Torr. Over this range in pressure, the trapped decay switches from Doppler controlled to impact collisional controlled. In the transition region between Doppler and collisional, the natural line width would appear to be important, but the redistribution effect does not allow the trapping to be evaluated simply by adding the natural and collision widths within the Lorentzian line profile. The TH theory for a cylindrical geometry with the Huennekens-Colbert modifications agrees with the data to within 50% over the *whole* range. In fact it agrees better with the experimental data than the Post theory with frequency redistribution.[17]

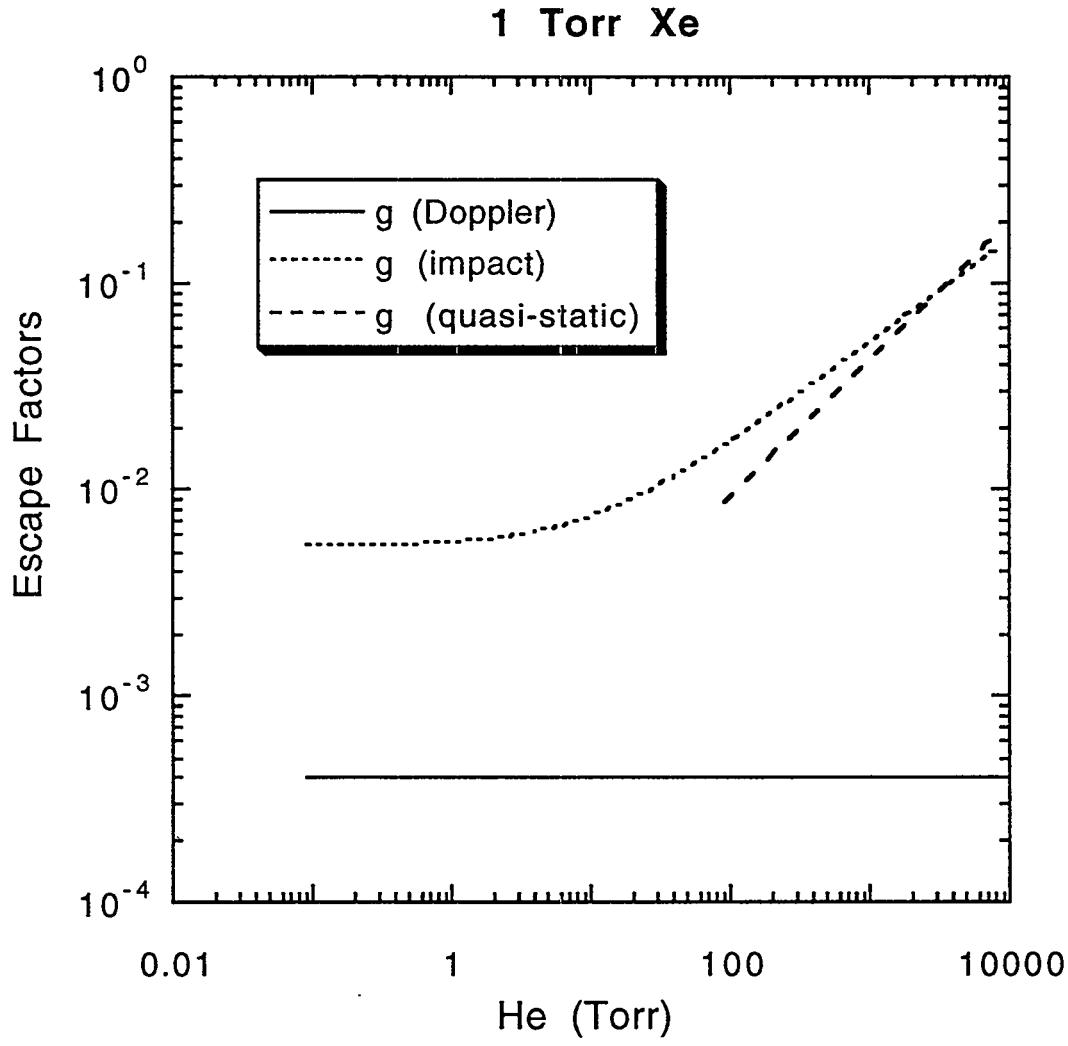

Figure 3. The escape factors, g(L), as a function of He pressure for 1 Torr of Xe. The characteristic length is 100 μm in the evaluation of the optical depth. "impact" refers to the impact limit of the total Xe plus He and Xe plus Xe broadening, while "quasi-static" refers to the quasi-static line shape of the Xe plus He system.

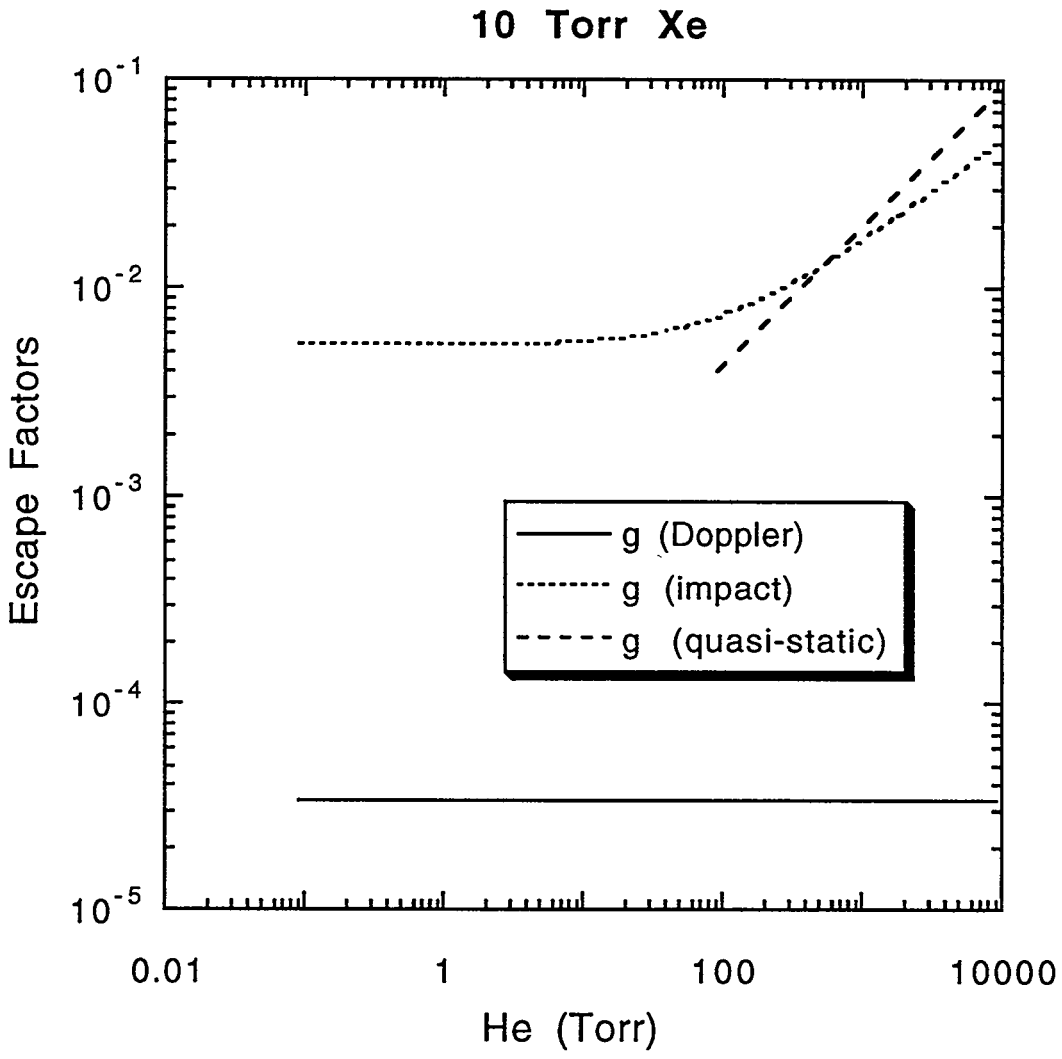

Figure 4. The escape factors, g(L), as a function of He pressure for 10 Torr of Xe. The characteristic length is 100 μm in the evaluation of the optical depth. "impact" refers to the impact limit of the total Xe plus He and Xe plus Xe broadening, while "quasi-static" refers to the quasi-static line shape of the Xe plus He system.

The numerical surveys presented in Figs. 1-4 indicate that the impact limit broadening of Xe by the "foreign" gas He and the resonance self-broadening of Xe by Xe combine to make the impact limit with its Lorentzian profile the only line broadening mechanism of importance from 1 Torr to almost 1000 Torr of total pressure in typical mixtures. For completeness, we give the necessary information to evaluate the trapping theory in the impact limit of pressure broadening for the 147 nm Xe line for most relevant situations in the He-Xe mixture. First of all the foreign (f) gas broadening must be specified; we have assumed a typical value for the coefficient:

$$\begin{aligned} &\Delta\omega_f = 2\pi\Delta\nu_f = 2\pi p_{He} B_{He,Xe}\,, \\ &B_{He,Xe} \approx 10\,MHz/Torr\,. \end{aligned} \tag{49}$$

The self or resonance (r) broadening is evaluated from the data of Carrington, Stacey, and Cooper.[15] They give:

$$\begin{aligned} &\Delta\omega_r = 2\pi n_l\, 2.407\beta\,, \\ &\beta = \frac{e^2}{4\pi\varepsilon_o}\frac{f_{osc}}{4m_e\omega_o}\,, \end{aligned} \tag{50}$$

where n_l is the number density of the lower (ground) level of Xe, 2.407 is a computed constant[15] for the appropriate kind of collisional process, e is the electron charge, m_e is the electron mass, and $f_{osc} \cong 0.28$ is the oscillator strength of the 147nm Xe transition.[16] The total pressure broadening is just:

$$\gamma_p = \Delta\omega_f + \Delta\omega_r\,, \tag{51}$$

which can be substituted directly into Eq.(11) to evaluate the line center extinction k_p. k_p is used in Eq. (13), or in Eqs.(12) and (46), to find the TH result for trapping in a slab or cylinder.

The space dependent decay rate as written in Eq.(44) is easily evaluated from the transmission function given in Eq.(12):

$$T_{ib}(s) = I_o(k_p\, s/2)\exp(-k_p\, s/2),$$
$$\approx \min\left(1, 1/\sqrt{\pi k_p s}\right), \tag{52}$$

where we introduced a bounding relation to enable the use of the asymptotic form of the Bessel function over the whole range of the argument. This is necessary for the space-dependent decay rate as one approaches a boundary surface of the active medium.

4. Discussion and Conclusion

This purpose of this report was to provide a tractable means of including radiation trapping within a computer simulation of plasmas relevant to the plasma flat panel display effort at Sandia National Labs and elsewhere. The immediate practical means of doing this is the Holstein (TH) theory, which has some limitations as we mentioned in the Introduction. The problem of lineshapes does not seem foreboding once we find that the impact-limit pressure broadening applies to nearly all of the parametric range of interest in these plasmas. Outside that range we would appeal to the Huennekens and Colbert[3] idea to combine Doppler and pressure broadening. The second and third limitations of the TH theory to the fundamental radiating spatial mode of a slab or cylinder have been addressed by a new approximation for obtaining a position-dependent decay rate for the trapped radiating level in the system. This approximation has not been implemented or tested numerically, but the analytic examinations indicate that it is close to the TH results when it should be. The diffusion approximation, which has numerical advantages over the use of the transport integrodifferential equation, does not appear to be useful by our analysis. As mentioned at the end of Section 2.2, an empirical definition of the diffusion constant to force it to agree with the TH decay rate may be the only way to make the diffusion approximation useful. This concept would need testing before implementation.

We can summarize the contents of this report by outlining the necessary programmatic steps for its complete implementation. The first step is to decide whether the TH theory with its assumed geometry is to be used, or whether the general space-dependent decay rate of Eq.(44) is to be used. One therefore begins with Eqs.(13) or (14), or Eq.(44), which are logically connected to T(s) in Eq.(52), which depends on k_p in Eq.(11), which needs γ_p from Eq.(51), which is a function of pressure and/or density as given in Eq.(49) and (50).

As one final point, we mention that the radiation escaping from the active plasma to the surface of the phosphor must be computed from the transmission function, *T(s)*. Thus one must have a representation of *T(s)* valid throughout the medium. The total radiation photon density E within the medium is evaluated from Eq.(1) by integrating over the spectral distribution of the emission line of interest. Although the emission is spectrally distorted, the absorption of the radiation by a phosphor will not be sensitive to the profile. The result is:

$$E(\vec{r},t)=\frac{\gamma_{sp}}{c}\int_V d^3r'\frac{T(s)}{4\pi s^2}n_u(\vec{r}',t),$$
$$s=|\vec{r}-\vec{r}'|. \tag{53}$$

which is to be evaluated when needed at the surface position of the phosphor. Note that this volume integral would have to be done to evaluate the radiation density whether one implements the TH decay rate or the space-dependent decay rate within the plasma simulation.

References

1. R. B. Winkler, J. Wilhelm, and R. Winkler, "Kinetics of the Ar-Hg Plasma of Fluorescent Lamp Discharges I. Model - Basic Equations- Hg Partial Pressure Variation," Annalen der Physik., **40**, 90-118 (1983).

2. R. B. Winkler, J. Wilhelm, and R. Winkler, "Kinetics of the Ar-Hg Plasma of Fluorescent Lamp Discharges II. Ar Partial Pressure and Discharge Current Variation," Annalen der Physik., **40**, 119-139 (1983).

3. J. L. Deschamps, in Proceedings of the Society for Information Display International Symposium, San Jose, California 1994, SID 94 Digest, p. 315 (1994).

4. T. Holstein, "Imprisonment of Resonance Radiation in Gases," Phys. Rev., **72**, 1212-1233 (1947).

5. T. Holstein, "Imprisonment of Resonance Radiation in Gases. II," Phys. Rev., **83**, 1159-1168 (1951).

6. J. Huennekens and T. Colbert, "On Radiative Transport of the Resonance Lines of Sodium," J. Quant. Spectrosc. Radiat. Transfer, **41**,439-446 (1988).

7. C. van Trigt, "Analytically Solvable Problems in Radiative Transfer. I," Phys. Rev., **181**, 97-114 (1969).

8. J. E. Lawler, G. J. Parker, and W. N. G. Hitchon, "Radiation Trapping Simulations Using the Propagator Function Method," J. Quant. Spectrosc. Radiat. Transfer, **49**, 627-638 (1993).

9. G. Vermeersch and W. Wieme, in *Optogalvanic Spectroscopy*, R. S. Stewart and J. E. Lawler, eds., Inst. of Physics Conf. Ser. No. 113, 109 (1991).

10. J. Huennekens, H. J. Park, T. Colbert, and S. C. McClain, "Radiation trapping in sodium-noble-gas mixtures," Phys. Rev. A, **35**, 2892-2901 (1987).

11. T. Colbert and J. Huennekens, "Radiation trapping in the far wings of the foreign-gas broadened potassium resonance lines," Phys. Rev. A, **44**, 4753-4755 (1991).

12. R. B. Campbell, Sandia National Labs, private communications.

13. F. E. Irons, I. "The Escape Factor in Plasma Spectroscopy - I. The Escape Factor Defined and Evaluated," J. Quant. Spectrosc. Radiat. Transfer, **22**, 1 (1979), "The Escape Factor in Plasma Spectroscopy - II. The Case of Radiative Decay," *ibid* **22**, 21 (1979), "The Escape Factor in Plasma Spectroscopy - III.Two Case Studies," *ibid* **22**, 37 (1979).

14. I. I. Sobel'man, "Introduction to the Theory of Atomic Spectra," Ch. 10, Pergamon Press, Oxford (1972).

15. C. G. Carrington, D. N. Stacey, and J. Cooper, "Multipole relaxation and transfer rates in the impact approximation: application to the resonance interaction," J. Phys. B: Atom. Molec. Phys. **6**, 417-432, (1973).

16. H. M. Anderson, S. D. Bergeson, D. A. Doughty, and J. E. Lawler, " Xenon 147-nm resonance *f* value and trapped decay rates," Phys. Rev. A, **51,** 211-217, (1995).

17. F. Vermeersch, N. Schoon, E. Desoppere, and W. Wieme, "Experimental investigation of the imprisonment of the ($^3P_1$–$^1S_0$) 146.96 nm resonance radiation in Xenon," in *Optogalvanic Spectroscopy*, R. S. Stewart and J. E. Lawler, eds., Inst. of Physics Conf. Ser. No. 113, 133-140 (1991).

DISTRIBUTION:

1 Dr. James Norman Bardsley
Mailcode L-296
Lawrence Livermore National Lab
P O Box 808
Livermore, CA 94550

1 Dr. Paul Drallos
Dept. of Physics and Astronomy
University of Toledo
Toledo, OH 43606

1 Professor David Graves
Department of Chemical Engineering
University of California
201 Gilman Hall
Berkeley, CA 94720

1 Professor Mark Kushner
Electrical and Computer Engineering
University of Illinois
Urbana, IL 61801

1 Professor William Williamson, Jr.
Dept. of Physics and Astronomy
University of Toledo
Toledo, OH 43606

1 MS 0834 Robert B. Campbell, 1512

1 MS 0827 Robert T. McGrath, 1511

1 MS 0740 Ramana Veerasingam, 6531

1 MS 9043 Ellen Meeks, 8745

1	MS 9043	Bob Kee, 8745
10	MS 1423	Merle Riley, 1128
1	MS 1423	W. J. Alford, 1128
1	MS 9018	Central Technical Files, 8523-2
5	MS 0899	Technical Library, 13414
1	MS 0619	Print Media, 12615
2	MS 0100	Document Processing, 7613-2 For DOE/OSTI